ACS OMEGA

ACS AuthorChoice

http://pubs.acs.org/journal/acsodf

Article

Experimental and Computational Investigations of Carboplatin Supramolecular Complexes

Sherif Ashraf Fahmy, Fortuna Ponte, Emilia Sicilia, and Hassan Mohamed El-Said Azzazy*

Cite This: *ACS Omega* 2020, 5, 31456−31466

Read Online

ACCESS | Metrics & More | Article Recommendations | Supporting Information

ABSTRACT: Supramolecular systems (macromolecules), such as calix[*n*]arenes (SCn), cyclodextrins (CDs), and cucurbiturils (CBs), are promising vehicles for anticancer drugs. In this work, guest−host complexes of carboplatin, a second-generation platinum-based anticancer drug, and p-4-sulfocalix[*n*]arenes (n = 4 and 6; PS4 and PS6, respectively) were prepared and studied using ^{1}H NMR, UV, Job's plot analysis, HPLC, and density-functional theory calculations. The experimental and the computational studies suggest the formation of 1:1 complexes between carboplatin and each of PS4 and PS6. The stability constants of the formed complexes were estimated to be 5.3×10^4 M^{-1} and 9.8×10^4 M^{-1}, which correspond to free energy of complexation of −6.40 and −6.81 kcal mol^{-1}, in the case of PS4 and PS6, respectively. The interaction free energy depends on the different inclusion modes of carboplatin in the host cavities. UV−vis findings and atoms in molecules analysis showed that hydrogen bond interactions stabilize the host−guest complexes without the full inclusion in the host cavity. The in vitro anticancer study revealed that both complexes exhibited stronger anticancer activities against breast adenocarcinoma cells (MCF-7) and lung cancer cells (A-549) compared to free carboplatin, preluding to their potential use in cancer therapy.

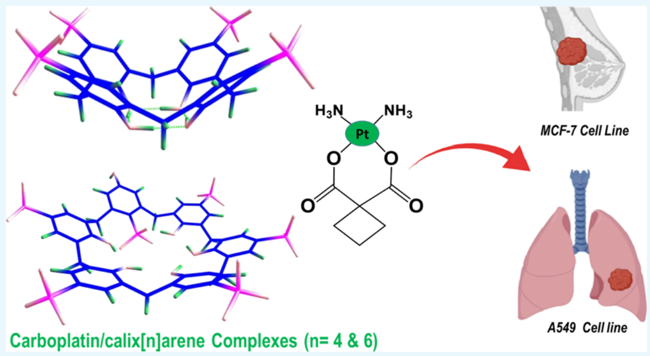

1. INTRODUCTION

Platinum-based chemotherapeutic drugs (PBDs) are potent broad-spectrum anticancer medicines used in chemotherapy of more than 50% of cancer patients.[1,2] Cisplatin (*cis*-diammine(dichloro)platinum(II)), a first-generation platinum complex, has significant broad-spectrum anticancer activities against a wide range of solid tumors, such as lung, cervical, ovarian, esophageal, uterine, and bladder.[1,2] Cisplatin has been approved by the US Food and Drug Administration (FDA) in the late 1970s. However, cisplatin administration has been accompanied by many systemic side effects including ototoxicity, nephrotoxicity, neurotoxicity, and emetogenesis. Additionally, cisplatin treatment is limited by intrinsic and acquired resistance presented by many tumor cells following repeated treatment regimens.[1−3]

Consequently, newer generations of PBDs have been developed to increase anticancer activities and reduce systemic toxic effects.[1−5] Carboplatin (*cis*-diammine(1,1-cyclobutanedicarboxylato)platinum(II) was developed as a second-generation PBD and was granted FDA approval as a safer alternative to cisplatin, with negligible neurotoxicity and ototoxicity and reduced renal toxicity and emetogenesis.[3−5] Carboplatin exerts its antitumor activity, similarly to cisplatin, via aquation and formation of activated aquated species interacting with the DNA of cancer cells, forming Pt-DNA adducts leading to apoptosis.[6,7]

Both cisplatin and carboplatin have similar chemical structures, but they differ in their leaving groups, which are dichloride ligands in cisplatin and cyclobutane-1,1-dicarboxylate ligand in carboplatin (Figure S1). This structural modification imparts a more tolerable toxicity profile to carboplatin. However, frequent administration of carboplatin results in severe thrombocytopenia and myelosuppression. Because carboplatin has a similar chemical structure to cisplatin, it exhibits similar activity spectrum and resistance. This has limited the use of carboplatin in treating cisplatin-resistant cancers.[6−9]

Various mechanisms are responsible for developing PBD drug resistance such as reducing the intracellular accumulation of drugs by reducing influx or increasing efflux or detoxifying the chemotherapeutic agent by biomolecules containing thiol groups. Other mechanisms include intonation of downstream signaling pathways or inhibiting apoptosis. Hence, significant efforts have been exerted to develop novel approaches to overcome the limitations of PBDs. In this context, PBDs have

Received: October 23, 2020
Accepted: November 13, 2020
Published: November 25, 2020

https://dx.doi.org/10.1021/acsomega.0c05168
ACS Omega 2020, 5, 31456−31466

been partially or fully encapsulated into drug delivery vehicles such as PEGylated liposomes, niosomes, polymeric nanocomposites, and dendrimers.[9−15]

More recently, supramolecular systems (macrocycles), including calix[n]arenes (CXs), cyclodextrins (CDs), cucurbiturils (CBs), and pillararenes, have drawn attention as potential carriers for PBDs via either host−guest complexation or self-assembly.[16−20]

Some previous studies reported the possible use of supramolecular host molecules as promising carriers for PBDs to enhance their water solubility, chemical stability, and bioavailability.[16] The host−guest complexation could also improve the selective delivery of chemotherapeutics to cancer cells, resulting in improved anticancer activities with minimal toxic systemic effects.[16−20] Host−guest complexation between PBDs and host supramolecular systems might reduce systemic side effects and resistance and improve the complex's anticancer activity compared to the free drug.[16−20] For instance, the host−guest complexation between cisplatin and cucurbit[7]uril (CB7) stabilized through four hydrogen bonds reduced systemic adverse effects and overcame cancer cell resistance by modifying the pharmacokinetic profile of cisplatin in the blood circulation.[20] Another study reported reducing oxaliplatin's toxic effects and enhancing its anticancer activity against leukemia cancer cells (L1210FR) upon its host−guest complexation with CB7 at significantly lower concentrations than the free drug.[17]

CXs, in specific, have attracted much attention as significant host molecules that have been used in many fields of supramolecular chemistry. CXs (n = 4, 6, and 8) are cone-shaped cyclic oligomers composed of phenol units connected by methylene bridges. CXs have a unique structure that comprises an upper rim with a para-substituent of a phenolic ring, a lower rim with a phenolic hydroxyl group, and a hydrophobic π electron-rich core cavity. Thus, they are excellent host molecules for various therapeutically active guest molecules. The water solubility of CXs is improved by adding some functional groups, such as carboxylates and sulfonates, at the para-position of their phenolic units.[16,21,22] *Para*-sulfonato-calix[n]arenes [n = 4 and 6, (PS4 and PS6)] exhibited remarkable water solubility (>0.1 mol/L). More importantly, they are biocompatible and nontoxic to human cells as they show no in vitro hemolysis at doses up to 5×10^3 μM. However, they may cause minimal systemic toxicity in vivo at doses up to 10^4 μg/Kg. Owing to their π-rich cavities, *para*-sulfonato-calix[n]arenes in aqueous media were used to accommodate active guest molecules.[21,22]

This work investigates the complexation between either PS4 or PS6 and carboplatin in aqueous media for potential use in cancer therapy. Experimental and theoretical studies of the host−guest complexation between PS4 or PS6 and carboplatin in aqueous media were conducted for potential cancer therapy applications. The formed complexes have been characterized by UV−vis spectrophotometry and ^{1}H NMR spectroscopy. The stoichiometry and binding constants were detected employing Job's plot (continuous variation method) and HPLC. The derivative ratio method was utilized to eliminate the interference caused by the overlapped host spectra. Moreover, the anticancer activities of both complexes against breast adenocarcinoma cells (MCF-7) and lung cancer cells (A-549) were evaluated using sulforhodamine B colorimetric assay (SRB assay). Density-functional theory (DFT) calculations were carried out to obtain structural information on the inclusion of carboplatin into the cavities of the examined calixarenes and binding energies for the host−guest (1:1) formed complexes. The intermolecular hydrogen bonds for all the intercepted adducts were investigated utilizing Atoms in Molecules (AIM) analysis.

2. RESULTS AND DISCUSSION

2.1. ^{1}H NMR Spectroscopy. ^{1}H NMR measurements in D_2O were performed to study the complexation between carboplatin and either PS4 or PS6. The ^{1}H NMR findings revealed that carboplatin protons had not displayed remarkable shifts upon adding PS4 (Figure S2 and Table 1). The signal for the protons of the two doublet 4H and the triplet 2H of the methylene groups in the cyclobutane ring of carboplatin, Ha and Hb, respectively (Figure S2 and Table 1), demonstrated small chemical shifts of 0.045 and 0.094 ppm, respectively. This shows that these protons are not fully embedded inside the PS4 cavity. Previous studies reported the direct relationship between the extent of the chemical shift of the protons of a guest molecule and the depth of these protons inside the hollow cavity of the host macromolecule.[23−25] However, we observed that the signal of the methylene bridge protons, Hy, of the 1:1 M ratio mixture of PS4 and carboplatin, showed remarkable broadening compared with the same signal in PS4 alone (Figure S2). This signal widening indicates the macromolecule host structure's conformational rigidity induced by its complexation with the carboplatin guest molecule.[23,26] The complexation of oxaliplatin with PS6 exhibited a similar behavior. These exciting findings suggest that there is complexation, due to bond formation (hydrogen bonds as evidenced from the theoretical investigation below), between carboplatin and either PS4 or PS6 but without involving the embedding of CH_2 protons (of the cyclobutane nucleus of carboplatin) inside the hollow cavities of either PS4 or PS6. This complex was further evaluated by UV−vis spectroscopy and HPLC.

Table 1. Detected Shielding (ppm) for Allocated Protons in Carboplatin, PS4, and 1:1 M Ratio Carboplatin to PS4 in D_2O

proton signals	individual molecules	1:1 M ratio
Hz[a]	7.353	7.355
Hy[a]	4.081	4.091
Ha[b]	2.657	2.612
Hb[b]	1.643	1.737

[a]Protons of PS4 (Figure S2). [b]Protons of Carboplatin (Figure S2).

2.2. UV−Vis Spectroscopy. Figure S3 depicts the UV absorbance spectra of 0.2 mM carboplatin, 0.2 mM PS4, and mixtures encompassing increasing carboplatin concentrations (ranging from 0.01−0.21 mM) and 0.2 mM PS4 all in aqueous media. The same procedure was followed using PS6 instead of PS4 (Figure S3). Carboplatin exhibited weak absorbance through the wavelength in the range of 245−310 nm (Figure S3). However, it is evident that the spectrum of either PS4 or PS6 showed noticeable absorption maxima at 277 and 284 nm (Figure S3). The spectra of the mixtures (prepared using PS4 or PS6) displayed a significant hyperchromic shift, which was associated with increasing carboplatin concentration. Additionally, the characteristic pair of absorption maxima for either PS4 or PS6 was reserved without any merging, and no remarkable red or blue shifts took place. This suggests that most probably, the complex formed between carboplatin and either PS4 or PS6 does not involve full penetration of the guest molecule within the cavity of the host macromolecule (the complex formed is not an inclusion complex). This was evidenced by previous studies that observed the merging of the host's characteristic pair of maxima and the appearance of new maxima specific for the inclusion complex.[23]

The hyperchromic shift observed with increasing concentrations of carboplatin was studied using our previously reported methods.[23] The zero-order spectra of the prepared mixtures were divided by the spectrum of PS4, and the first derivative of the ratio spectra was found using a scaling factor of 10 and $\Delta\lambda$ = 4 nm.[23] The values of the peak amplitudes of the first derivative of the ratio spectra for the mixtures were then obtained at 266 nm. Figure 1A depicts a plot of the attained peak amplitudes and

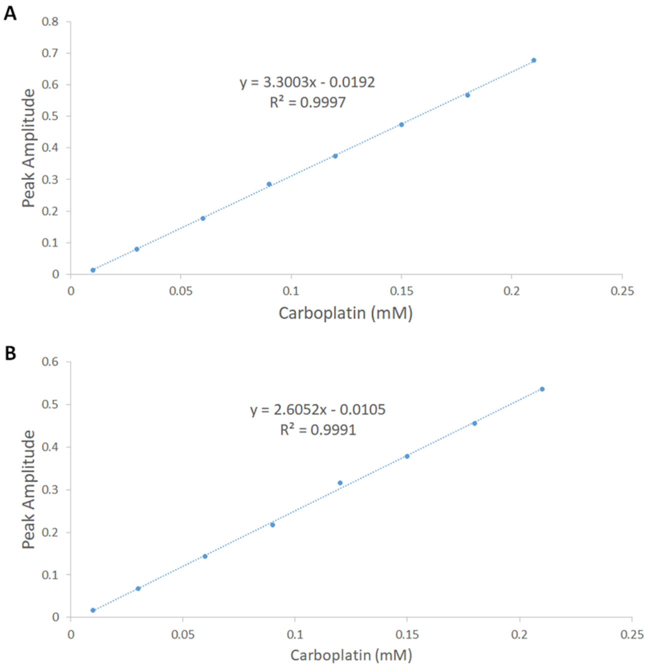

Figure 1. Plot of peak amplitudes at 266 nm obtained from the mixtures containing consecutively increasing concentrations of carboplatin (0.01−0.21 mM) and a fixed concentration of (A) 0.2 mM PS4 and (B) 0.2 mM PS6.

the corresponding concentrations of carboplatin. The consecutive addition of increasing carboplatin concentrations to a fixed concentration of PS6 has resulted in a similar behavior. A plot of the acquired peaks in carboplatin/PS4 and the equivalent concentrations of carboplatin are depicted in Figure 1B. The ideal linear relationships depicted in Figure 1 suggested that the hyperchromic shifts observed in carboplatin/PS4 and carboplatin/PS6 are attributed to a complex formation between carboplatin and each of PS4 (Figure 1A) and PS6 (Figure 1B).

The stoichiometry and the stability constants of the supramolecular complexes were investigated using Job's plot (the method of continuous variation) involving the derivative ratio method, using methods described previously.[23] From Job's plots, we observed that the maximum amplitudes were detected at molar fractions of 0.5, indicating a host−guest complex stoichiometry of 1:1 for carboplatin/PS4 and carboplatin/PS6. A normalized form of these Job's plots for carboplatin/PS4 and carboplatin/PS6, where each of the amplitude values, S, were divided by the equivalent maximum amplitude, S_{max}, is shown in Figure 2A,B, respectively. The stability constants of the complexes detected using methods described previously[23,27−29] were found to be 5.3 × 10^4 M^{-1} and 9.8 × 10^4 M^{-1}, which correspond to complexation free energy of −6.4 and −6.81 kcal

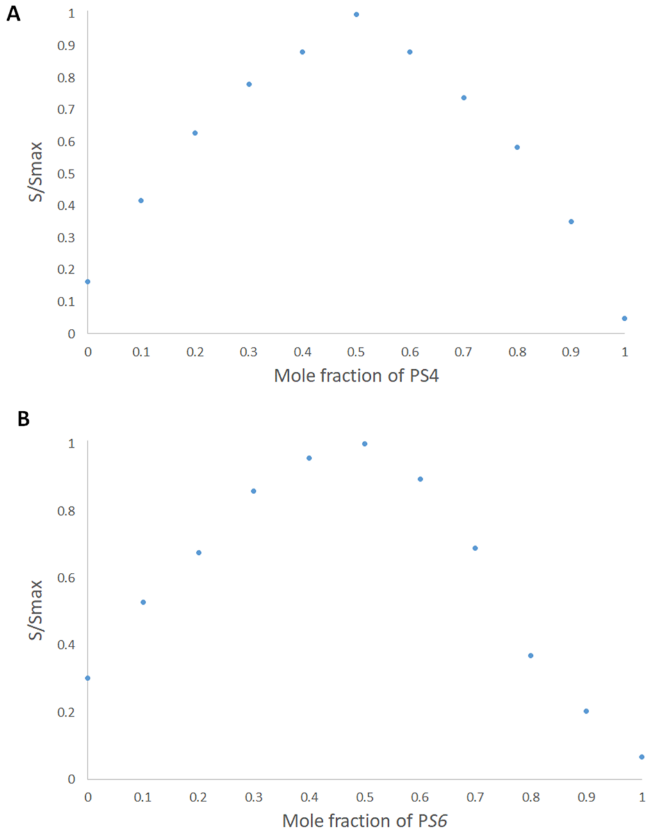

Figure 2. Normalized Job's plot: (A) PS4/carboplatin complex and (B) PS6/carboplatin complex.

mol^{-1}, for carboplatin/PS4, and carboplatin/PS6, respectively. These values are in line with the stability constants (0.01 × 10^3 to 1.7 × 10^5 M^{-1}) formerly reported for supramolecular complexes intended to be used for drug delivery purposes, and many of them showed improved pharmacokinetics, chemical stability, and more significant biological actions.[23,30−41]

2.3. HPLC. HPLC coupled with a photodiode array detector has been used to investigate the complexation between carboplatin and each of PS4 and PS6. A photodiode array detector facilitated the simultaneous detection of carboplatin at 210 nm and each of PS4, PS6, and their complexes with carboplatin at 266 nm. The chromatographic conditions involved the use of Column C18 Scharlau (1 cm × 25 cm, 5 μm), mobile phase composed of water and acetonitrile (99:1), a flow rate of 1.2 mL/min, temperature of 40 °C, and isocratic elution mode. At a fixed concentration of carboplatin, its detected signal was found to weaken with increasing concentrations of each of PS4 and PS6. This indicated that carboplatin formed a complex with PS4 and PS6, in line with our discussion mentioned earlier. This led us to test some solutions of varying molar ratios of carboplatin and each of PS4 and PS6, where the former was fixed at 0.05 mM, and the latter was allowed to vary from 0.01 to 0.09 mM, as presented in Figure 3. In Figure 3A,B, carboplatin (0.05 mM) was not observed when PS4 and PS6 existed in the range of 0.09−0.06 mM. This indicates that at these molar ratios, almost all the carboplatin in these solutions was complexed with PS4 and PS6. Additionally, Figure 3 shows a signal for carboplatin to be detected initially only when equal molar ratios of 0.05 mM for each carboplatin, PS4, and PS6 were present in the medium, indicating a 1:1 carboplatin to PS4 and PS6 complexation as discussed

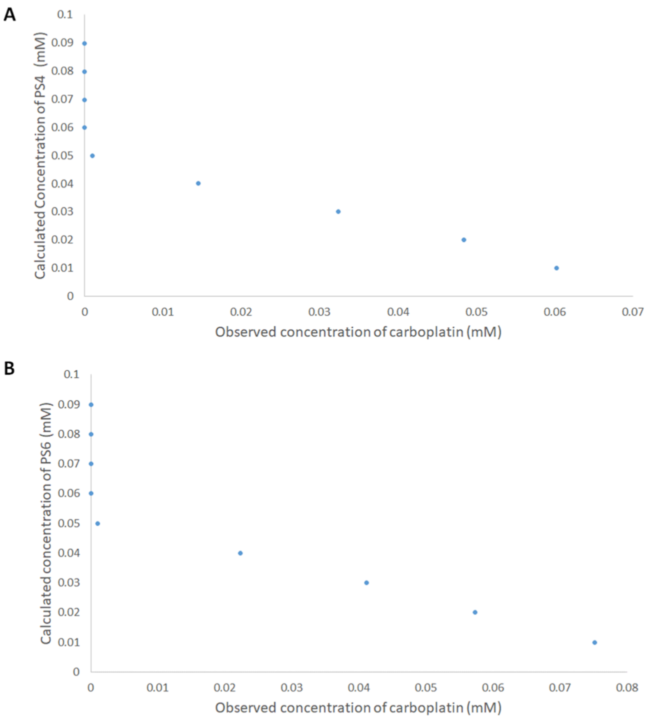

Figure 3. HPLC determined concentrations of carboplatin of solutions containing a fixed 0.05 mM of carboplatin and varying concentrations of (A) PS4 and (B) PS6 (0.01−0.09 mM).

previously. The stability constants of PS4/carboplatin and PS6/carboplatin complexes were calculated, as reported previously,[23] to be 4.8×10^4 M^{-1} and 8.8×10^4 M^{-1}, respectively, which is in line with the stability constants estimated from Job's plot.

2.4. In Vitro Cell Viability Assay. The anticancer activities of PS4, PS6, carboplatin, PS4/carboplatin, and PS6/carboplatin were tested on breast adenocarcinoma cells (MCF-7) and lung cancer cells (A-549) using SRB assay. Both PS4 and PS6 were utilized as host control, where they both exhibited no significant decrease in cell viability. Our observations show that both complexes have significant in vitro anticancer activities compared to free drug. The anticancer activities (IC50 in μg/mL, computed by Sigma plot, as detailed earlier) of PS4, PS6, carboplatin, PS4/carboplatin, and PS6/carboplatin against both cell lines are presented in Table 2. The IC50 of both complexes exhibited almost twice that of the free carboplatin against MCF-7 cells, while the IC50 of PS4/carboplatin and PS6/carboplatin against A-549 displayed about four-times and ten-times that of free drug, respectively. The increased anticancer activities of both complexes compared to free carboplatin might be due to their enhanced water solubility, and hence bioavailability, of the drug upon complexation with PS4 and PS6.[42,43]

These preliminary findings are very promising and support the use of the developed complex for a possible reduction of the therapeutic dose of carboplatin, which consequently will decrease the toxic side effects. Alternatively, clinicians may choose to use a higher dose of carboplatin in the designed complex to boost cancer therapy.

2.5. Computational Studies. The optimized structures of the *para*-sulfonato-calix[4]arene (PS4) in cone conformation and the PS6 in the partial cone conformation are shown in Figure 4.[44]

The PS4 is characterized by upper and lower rim distances of 9.416 and 5.308 Å, respectively, and intramolecular H-bonds between the OH groups stabilize the conformation. Such a conformation suggests that the entrance of a guest molecule into the cavity through the upper rim is viable. The investigated PS6 conformation exhibits a less symmetric cavity structure than the cone conformation, stabilized by the circular H-bonds between the hydroxyl groups, and the weak interactions determine its stability. The protonated sulfonate groups, in this conformation, are linked via hydrogen bonds, causing the deformation and closure of the calixarenes.

As shown recently,[45] it is possible to predict the penetration of a guest molecule into the host's cavity based on their volumes. The van der Waals surface graph, obtained by the intersection of the atomic van der Waals spheres, is reported in Figure S4 and shows the maximum distances in height, length, and width describing carboplatin's size with a total volume of 176 Å^3.

The calculated carboplatin volume indicates its potential inclusion into the PS4 and PS6 cavities, which exhibit inner volumes of 587 and 994 Å^3, respectively. Moreover, on comparing the van der Waals surfaces of carboplatin with the dimension of the symmetric PS4, its inclusion within the cavity may be possible. However, several factors must be taken into account in the formation of the host−guest inclusion complexes. All the possible insertion scenarios, computationally investigated, of the carboplatin drug into the cavity of PS4 and PS6 are reported in Scheme 1. The inclusion of carboplatin into the examined calixarenes was simulated from both the upper rim (**U**) side and the side of the lower rim (**L**). Also, carboplatin can be inserted inside both the cavities assuming two different orientations. Label (**a**) depicts the arrangement in which the ammonia ligands point toward the interior of the cavity and the cyclobutane ring points outside, while in (**b**), the cyclobutane ring points toward the inside of the cavity and the ammonia ligands are externally oriented.

The fully optimized geometries obtained without imposing any constraint for these host−guest complexes, together with the most significant geometrical parameters and the values of the complexation free energies calculated including basis set superposition error (BSSE) and entropy change corrections in solution, are reported in Figure 5 for the complexes formed with PS4 and in Figure 6 for PS6 complexes. Many attempts have been carried out, adopting different reciprocal orientations between the hosts and the guest that collapse into the reported optimized structures.

For PS4 calixarene host, carboplatin can assume both (**a**) and (**b**) orientations, for the inclusion from the upper side, obtaining

Table 2. In Vitro Anticancer Activities of PS4, PS6, Carboplatin, PS4/Carboplatin, and PS6/Carboplatin against Two Different Cancer Cell Lines

	in vitro anticancer activity (IC50 in μg/mL)				
cells	PS4	PS6	carboplatin	PS4/carboplatin	PS6/carboplatin
MCF-7	N/A	136	9.5	4.3	3.8
A-549	>300	136	23	5	2.1

https://dx.doi.org/10.1021/acsomega.0c05168
ACS Omega 2020, 5, 31456−31466

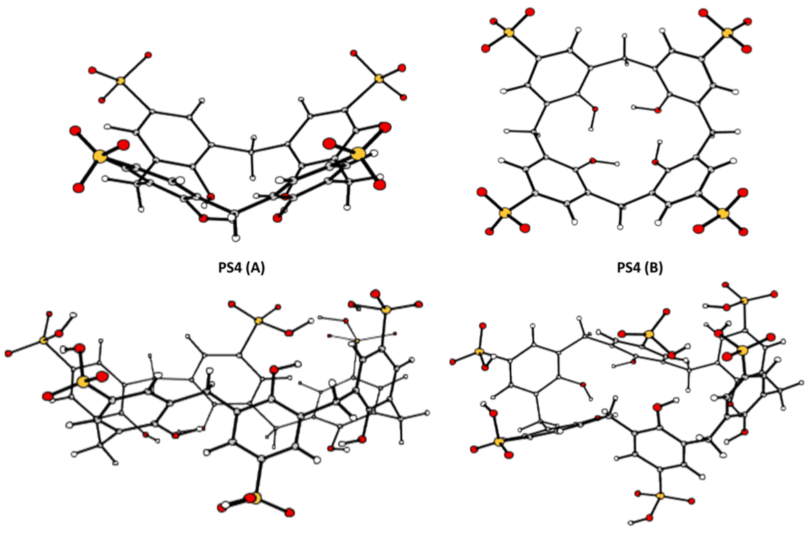

Figure 4. Optimized structures of PS4 and PS6 shown in two projections: (A) side view and (B) top view. The three-dimensional images of the optimized structures were prepared using CYLview Visualization Software.[44]

Scheme 1. Investigated Possible Inclusion Modes of Carboplatin through the Upper (U) and Lower (L) Rims of PS4, Indicated as 1, and PS6, Indicated as 2[a]

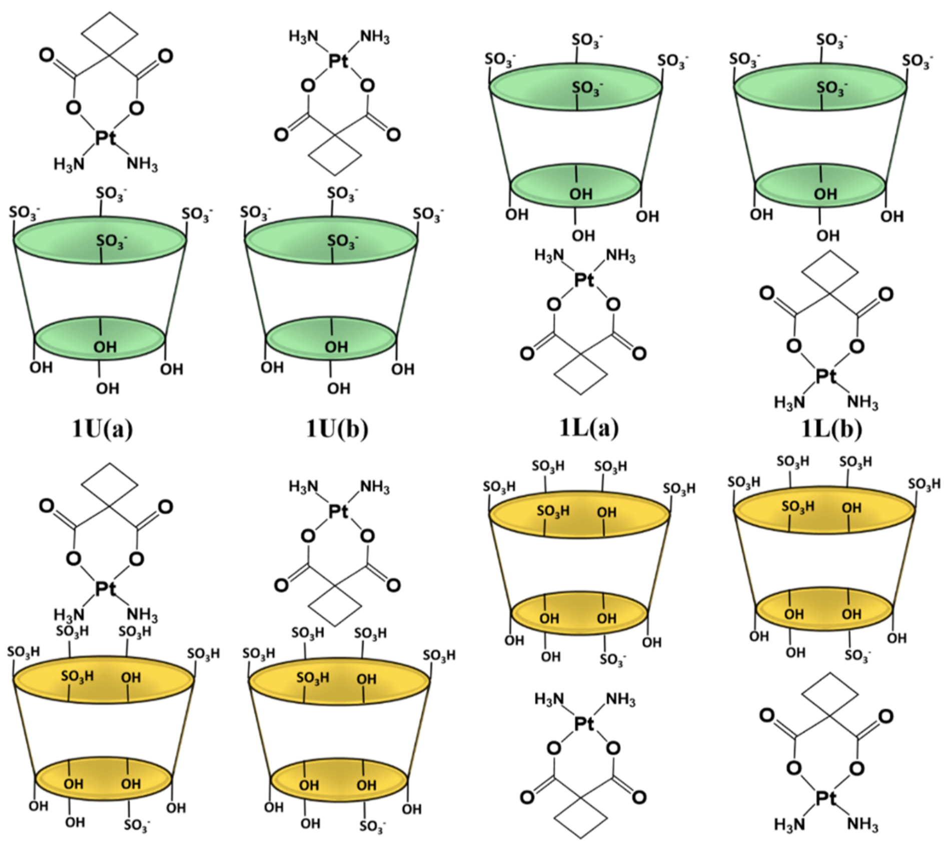

[a]In **U(a)** configuration, the ammonia ligands point toward the inside of the upper rim of the cavity and the cyclobutane outward. In **U(b)** configuration, the cyclobutane point toward the inside of the upper rim of the cavity and the ammonia ligands outward. In **L(a)** configuration, the ammonia ligands point toward the inside of the lower rim of the cavity and the cyclobutane outward. In **L(b)** configuration, the cyclobutane point toward the inside of the lower rim of the cavity and the ammonia ligands outward.

type **U(a)** and **U(b)** conformations. These structures are here reported as **1U(a)**$_1$, **1U(a)**$_2$, and **1U(b)**. Although an attempt to include carboplatin starting from orientation **(b)** was carried out, during the optimization, the orientation of the complex with respect to calixarene changed, and the optimized geometry collapsed into the **1U(a)**$_2$ configuration. In the optimized **1U(b)**

https://dx.doi.org/10.1021/acsomega.0c05168
ACS Omega 2020, 5, 31456−31466

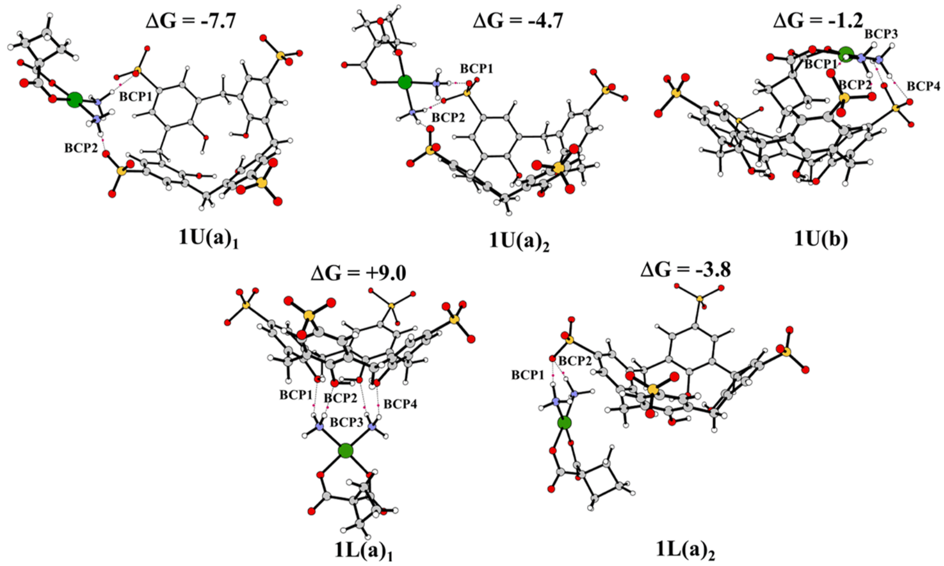

Figure 5. B97-D optimized geometrical structures of PS4, bond critical points (BCPs) present and binding energies (kcal mol^{-1}). The three-dimensional images of the optimized structures were prepared using CYLview Visualization Software.[44]

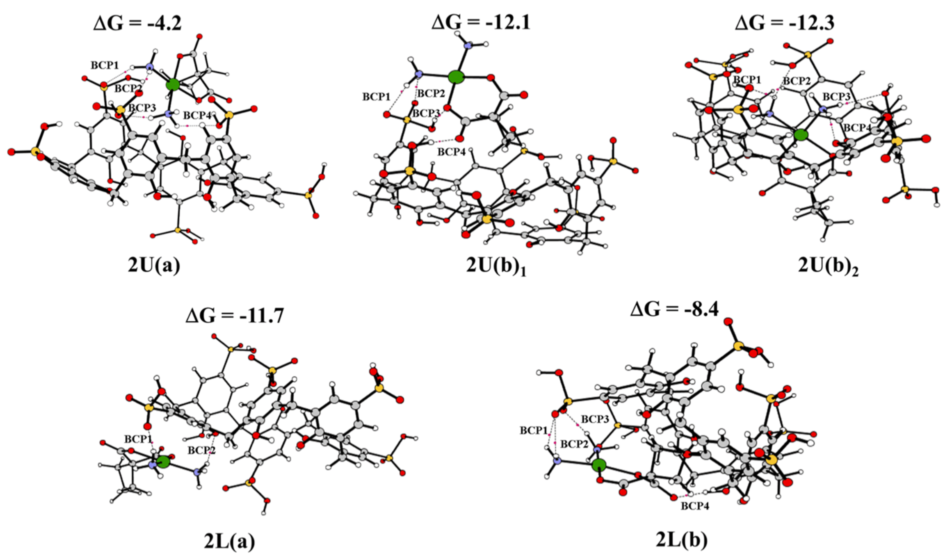

Figure 6. B97-D optimized geometrical structures of PS6, BCPs present and binding energies (kcal mol^{-1}). The three-dimensional images of the optimized structures were prepared using CYLview Visualization Software.[44]

adduct, carboplatin was manually included in the calixarene in the host−guest model reported in Figure 5. For the inclusion from the lower side, only the arrangements of (**a**) type converged, obtaining two **L**(**a**) conformations indicated as $\mathbf{1L(a)_1}$ and $\mathbf{1L(a)_2}$. In all the intercepted structures, carboplatin prefers interacting with the cavity through the ammonia ligands' hydrogen atoms. In all the systems having an (**a**) arrangement, the guest remains outside the macrocycle. In the host−guest complex labeled **1U**(**b**), the carboplatin occupies the center of the cavity with the cyclobutane pointing inward, while the NH_3 ligands establish H-bond interactions with the oxygen atoms of the nearest sulfonate groups. Such complexes are characterized by a computed binding energy of −7.7, −4.7, −1.2, +9.0, and −3.8 kcal mol^{-1} for conformations $\mathbf{1U(a)_1}$, $\mathbf{1U(a)_2}$,**1U**(**b**), $\mathbf{1L(a)_1}$ and $\mathbf{1L(a)_2}$, respectively. The adduct in $\mathbf{1L(a)_1}$ configuration is found to be 9.0 kcal mol^{-1} higher in energy with respect to the isolated molecules. In that case, the guest lies under the cavity with the hydrogen atoms of the two NH_3 groups interacting with the O atoms of the OH groups. The guest−host interactions destabilize the original host structure by varying the charge distribution, leading to a destabilization of the system. However, except for the $\mathbf{1L(a)_1}$ configuration, the guest interacts with both ends of the host, maximizing the stabilizing forces. Even if all the computationally found configurations can be plausible, the best agreement is obtained with the $\mathbf{1U(a)_1}$ configuration. Indeed, its complexation energy is in accordance with the experimentally estimated free energy of complexation reported above, which corresponds to the value of −6.4 kcal mol^{-1}.

As reported in Figure 6, for the inclusion of the guest from the upper side into PS6 calixarene host, both (**a**) and (**b**) arrangements are feasible. Despite the different initial reciprocal positions of the host and the guest, carboplatin, in this case, chooses to interact through the hydrogen atoms of the ammonia ligands with the PS6 cavity. In both the intercepted structures, named $\mathbf{2U(a)_1}$ and $\mathbf{2U(b)_1}$, carboplatin is located outside the

Table 3. Characteristics of (+3, −1) BCPs Obtained from AIM Analysis for the Host−Guest Inclusion Complexes.[a]

conformation	BCP	ρBCP	$\Delta^2\rho$BCP	conformation	BCP	ρBCP	$\Delta^2\rho$BCP
1U(a)$_1$	1	0.0440	0.1179	1U(a)	1	0.0212	0.0604
					2	0.0193	0.0577
	2	0.0364	0.0952		3	0.0279	0.0774
					4	0.0114	0.0420
1U(a)$_2$	1	0.0292	0.0818	1U(b)$_1$	1	0.0139	0.0442
	2	0.0210	0.0660		2	0.0164	0.0457
	3	0.0321	0.0908		3	0.0500	0.1350
	4	0.0320	0.0873		4	0.0591	0.1470
1U(b)	1	0.0149	0.0450	1U(b)$_2$	1	0.0109	0.0378
	2	0.0289	0.0744		2	0.0164	0.0450
	3	0.0191	0.0521		3	0.0105	0.0389
	4	0.0231	0.0620		4	0.0194	0.0568
1L(a)$_1$	1	0.0230	0.0666	1L(a)	1	0.0262	0.0719
	2	0.0185	0.0561				
	3	0.0207	0.0612		2	0.0138	0.0422
	4	0.0216	0.0030				
1L(a)$_2$	1	0.0397	0.1034	1L(b)	1	0.0141	0.0478
					2	0.0157	0.0433
	2	0.0378	0.0994		3	0.0132	0.0459
					4	0.0532	0.1590

[a]BCP: Bond Critical Point; ρ: electron density (a.u.); ∇^2: Laplacian of electron density(a.u.).

host calixarene. The host−guest model in which carboplatin was forcibly included into PS4 was computationally simulated and indicated as **2U(b)$_2$**.

Both **(a)** and **(b)** arrangements were taken into consideration for the insertion from the lower side, by obtaining the systems identified as **2L(a)** and **2L(b)**. Carboplatin generally prefers interacting with the host cavity through the hydrogen atoms of the ammonia groups. In **2L(b)** configuration, the NH_3 groups are splayed outside the cavity and cyclobutane points inward. In this conformation, H-bond interactions between the carboxylic acid group of carboplatin and the protonated sulfonate moiety are formed.

The insertion of carboplatin into the PS6 cavity entails a significant deformation of the cavity, suggesting a stronger interaction of PS6 with the examined guest compared to PS4. Indeed, the calculated interaction free energies are −4.2, −12.1, −12.3, −11.7, and −8.4 kcal mol^{-1} for structures **2U(a)**, **2U(b)$_1$**, **2U(b)$_2$**, **2L(a)**, and **2L(b)**, respectively. Computational outcomes demonstrate that several host−guest complexes with PS6 may be plausible, and the carboplatin can interact from both U and L sides of the PS6 calixarene host, and only H-bonds determine their stability.

Moreover, the computationally obtained order of stability for the complexation between carboplatin and either PS4 or PS6 is in agreement with that observed experimentally.

The nature of the molecular interactions in the host−guest complexes was investigated using the AIM tool.[46] According to Bader and Essén, the electronic density value at the BCP—ρBCP and its Laplacian—$\nabla^2\rho$BCP determines the nature and the strength of the interactions.[47] In particular, for weak interactions such as van der Waals and hydrogen bonding, $\rho(r)$ is quite small. $\rho(r)$ is $\sim 10^{-2}$ a.u. or less for H-bond and 10^{-3} a.u. for van der Waals interactions, while the corresponding Laplacian $\nabla^2\rho(r)$ is positive in both the cases. The electron density and the Laplacian values calculated at the BCPs are reported in Table 3.

For all the complexes composed of carboplatin and the host PS4, the electron density values fall in the expected range (0.0149−0.0400 a.u.) for H-bonds,[48] and the sign of Laplacian of electron density is positive. The strength of these hydrogen bonds in carboplatin-PS4 adducts is verified by the highest positive values of the Laplacian. The most stable complex with carboplatin, **U(a)$_1$** configuration, characterized by a complexation energy of −7.7 kcal mol^{-1}, presents the critical points indicated as BCP1 and BCP2, which correspond to stronger interactions than those existing in all the presented systems. The values of Laplacian are 0.1179 a.u. for BCP1 and 0.0952 a.u. for BCP2. The bond lengths of the NH···O−S bonds correlating to BCP1 and BCP2 are equal to 1.735 and 1.819 Å, respectively.

In the host−guest complexes formed with the PS6 macrocycle, the range of variation of the electron density is 0.0114−0.0800 a.u. and the Laplacian values are positive. For PS6, the most stable configuration, excluding that in which carboplatin was manually included, is **2U(b)$_1$** with a binding energy of −12.1 kcal mol^{-1}. The kind of interaction established in such complexes is considered the strongest interaction due to the highest positive values of the Laplacian. In the complex, four critical points corresponding to H-bonds are observed, indicated as BCP1, BCP2, BCP3, and BCP4, defined by the corresponding values of Laplacian of 0.0442, 0.0457, 0.1350, and 0.1470 a.u., respectively. The bond lengths relative to BCP3 and BCP4 are very short and are equal to 1.660 and 1.593 Å, respectively. These bond formations help in increasing the stability of the complex.

3. CONCLUSIONS

Several techniques were used to investigate and characterize the supramolecular systems formed between either PS4 or PS6 calixarenes and carboplatin in aqueous media. UV−visible spectroscopy, ^{1}H NMR spectroscopy, Job's plot analysis, HPLC and DFT calculations were employed and suggested the formation of 1:1 complexes. The stability constants for the formed complexes were estimated to be 5.3×10^4 M^{-1} and 9.8×10^4 M^{-1}, which correspond to free energy of complexation of −6.40 and −6.81 kcal mol^{-1}, in the case of PS4 and PS6, respectively, while the interaction free energy theoretically calculated depends on the different inclusion modes of carboplatin in the host cavities. Depending on the insertion mode, different types of interactions are involved, and their calculated binding energies have the same order of magnitude as those experimentally estimated. Moreover, computational outcomes supported the same stability order obtained experimentally. In all the intercepted structures, the anticancer drug was not fully included within the host cavity. This outcome was also confirmed by UV−vis analysis, and according to the AIM analysis, hydrogen bond interactions stabilize the host−guest complexes. This combined study contributes to ascertain the presence in solution of stable complexes between carboplatin and PS4/PS6 macromolecules, possibly preluding to their use as drug delivery systems.

4. EXPERIMENTAL AND COMPUTATIONAL DETAILS

4.1. Chemicals and Reagents. Carboplatin and *para*-sulfocalix[4]arene, PS4, were obtained from BLD Pharmatech Co., Limited, Cincinnati, Ohio, USA. *Para*-sulfocalix[6]arene, PS6, was purchased from WuXi LabNetwork, China. Deuterium oxide and HPLC grade water were purchased from Sigma-Aldrich. Streptomycin, penicillin, fetal bovine serum, trichloroacetic acid (TCA), Dulbecco's Modified Eagle's Medium (DMEM) SRB, and tris(hydroxymethyl)aminomethane (TRIS) were purchased from Lonza, Basel, Switzerland.

4.2. Instrumentation. UV spectrophotometric measurements were conducted on a CARY 500 UV−vis−NIR Scan dual-beam spectrophotometer (Varian, Palo Alto, California, USA). ^{1}H NMR spectra were measured on a 400 MHz NMR Varian Mercury console spectrometer (Varian, Palo Alto, California, USA). HPLC measurements were carried out on a Waters 2690 Alliance HPLC system equipped with a Waters 996 photodiode array detector (Waters, Milford Massachusetts, USA.)

4.3. Cell Viability Assay. *4.3.1. Cell Culture.* Breast adenocarcinoma cells (MCF-7) and lung cancer cells (A-549) were obtained from American Type Culture Collection, (University Boulevard, Manassas, VA 20110, USA) and maintained in DMEM medium supplemented with streptomycin (100 mg/mL), penicillin (100 units/mL), and 10% heat-inactivated fetal bovine serum. Cells were incubated in 5% (v/v) CO2 at 37 °C.

4.3.2. Sulforhodamine B Colorimetric Assay. Breast adenocarcinoma cells (MCF-7) and lung cancer cells (A-549) were treated with different concentrations of PS4, PS6, carboplatin, PS4/carboplatin and PS6/carboplatin complexes. The preliminary in vitro anticancer activities of either MCF-7 or A-549 were tested using SRB assay.[49−51] Briefly, aliquots of 100 μL cell suspension (5×10^3 cells) were seeded in 96-well plates and incubated in DMEM medium for 24 h at 37 °C and 7% CO_2. Cells were treated with another aliquot of 100 μL medium containing different concentrations of PS4, PS6, carboplatin, PS4/carboplatin and PS6/carboplatin complexes (0.01, 0.03, 0.1, 0.3, 1, 3, 10, 30, 100, and 300 μg/mL). After 72 h, culture media were removed, and 10% TCA (150 μL) was added at 4 °C for 1 h. The cells were then washed several times with distilled water. SRB solution (70 μL; 0.4% w/v) was added and incubated for 10 min (dark at room temperature). Plates were washed three times with 1% acetic acid and permitted to dry overnight. The protein-bound SRB stain was then dissolved by adding 150 μL of 10 mM TRIS and absorbance measured at 540 nm (FLUOstar Omega, Ortenberg, Germany).

4.3.3. Calculation of IC50. Statistical analysis of IC50 values was computed from concentration−response curves by Sigma Plot software, version 12.0 (System Software, San Jose, CA, USA), using an *E*-max model equation

$$\%\ \text{cell viability} = (100 - R) \times \left(1 - \frac{[D]^m}{{K_d}^m + [D]^m}\right) + R \quad (1)$$

where (R) is the residual unaffected fraction (the resistance fraction), (D) is the drug concentration used, (K_d) is the drug concentration that produces a 50% reduction of the maximum inhibition rate, and (m) is a Hill-type coefficient. IC50 was defined as the drug concentration required to reduce absorbance to 50% of the control (i.e., K_d = IC50 when $R = 0$ and $E_{max} = 100 - R$). All experiments were performed in triplicate wells for each condition.

4.4. Computational Methods. Both the calixarene structures and their complexes with carboplatin were optimized by using Gaussian 09 suite of programs (Gaussian, Inc., Wallingford CT, 2009),[52] at DFT level employing the B97-D exchange and correlation functional.[53]

For the Pt atom, the Stuttgart/Dresden pseudopotential was used in conjunction with the corresponding split valence basis set.[54] The double-zeta 6-31G(d,p) basis set was used for all the atoms except oxygen, for which a diffuse function has been included. Similar systems have been successfully described using this computational protocol.[45]

Bulk solvent effects were considered by using the Tomasi's implicit Polarizable Continuum Model (PCM)[55] as implemented in Gaussian09. The solvation Gibbs free energies were calculated in the water dielectric environment ($\varepsilon = 78.4$) at the same level, performing single-point calculations on gas-phase optimized structures. Harmonic vibrational frequency calculations were performed to confirm the minimum character of the intercepted structures.

The Gibbs free energies for the inclusion of the carboplatin guest (G) into calixarene hosts (H), in implicit water, ΔG_{sol}, were calculated as the sum of two contributions: gas-phase free energy ΔG_{gas} and a solvation free energy ΔG_{solv}

$$\Delta G_{sol} = \Delta G_{gas} + \Delta G_{solv}^{H-Gcomplex} - (\Delta G_{solv}^{calix} + \Delta G_{solv}^{carboplatin})$$

where

$$\Delta G_{gas} = G_{gas}^{H-Gcomplex} - (G_{gas}^{carboplatin} + G_{gas}^{calix})$$

The binding energies were corrected for the BSSE by using the Boys−Bernardi counterpoise technique.[56]

In order to assess the potential inclusion of carboplatin into the calixarene cavities, the inner cavity volume was estimated by using Swiss-Pdb Viewer software.[57]

The types of molecular interactions between carboplatin and calixarenes, responsible for the formation of the adducts, were studied using the theory of AIM, recommended by Bader,[58] and the AIMAll program.[46] The AIM approach is based on the analysis of the electron density of molecular systems, $\rho(r)$, and is used to analyze the nature of chemical bonds. The electron densities of all the formed adducts were analyzed. The topological analysis of the molecular electron density, namely the analysis of the gradient of the $\rho(r)$, allows characterizing the chemical bonds and the so-called critical points (CPs), points at which the gradient is zero, that is $\nabla\rho(r) = 0$. The values of $\rho(r)$ and its derivatives at the CPs provide information about the nature and strength of the molecular systems' interactions under investigation. A total of 9 second-order derivatives of $\rho(r)$ are obtained, representing the elements of a real and symmetric

https://dx.doi.org/10.1021/acsomega.0c05168
ACS Omega 2020, 5, 31456−31466

Hessian matrix. The matrix can be diagonalized, by a unitary transformation, to obtain the corresponding eigenvalues (λ_n).

CPs are characterized by ω and σ, the rank, and the signature, respectively. The rank is given by the number of non-zero eigenvalues (non-zero curvatures of $\rho(r)$ at the CPs). The signature of a CP, instead, is the algebraic sum of the signs of eigenvalues (signs of curvatures of $\rho(r)$, the Laplacian $\nabla^2\rho(r)$, at the CPs). CP with $\omega = 3$ and $\sigma = +1$, corresponding to a (3, +1) CP, has two positive curvatures and ρ is a minimum at CP in the plane defined by their corresponding axes while at CP along the third axis, perpendicular to this plane, ρ is a maximum. The presence of a CP with $\omega = 3$ and $\sigma = -1$, corresponding to a (3, −1) CP, highlights that an accumulation of electronic charge density exists among the involved atoms; a chemical bond is formed. Such a point is denoted as a BCP.

ASSOCIATED CONTENT

Supporting Information

The Supporting Information is available free of charge at https://pubs.acs.org/doi/10.1021/acsomega.0c05168.

Chemical structures of cisplatin and carboplatin; [1]HNMR spectra of PS4, carboplatin alone, and the equimolar ratio of carboplatin and PS4; zero-order spectra of (A) PS4/carboplatin complex and (B) PS6/carboplatin complex at varying concentrations; and van der Waals surface graph for carboplatin (PDF)

AUTHOR INFORMATION

Corresponding Author

Hassan Mohamed El-Said Azzazy − *Department of Chemistry, School of Sciences & Engineering, The American University in Cairo, New Cairo 11835, Egypt*; Phone: +20-2-2615-2559; Email: hazzazy@aucegypt.edu

Authors

Sherif Ashraf Fahmy − *Department of Chemistry, School of Sciences & Engineering, The American University in Cairo, New Cairo 11835, Egypt*; orcid.org/0000-0003-3056-8281

Fortuna Ponte − *Department of Chemistry and Chemical Technologies, University of Calabria, Arcavacata di Rende 87036, Italy*

Emilia Sicilia − *Department of Chemistry and Chemical Technologies, University of Calabria, Arcavacata di Rende 87036, Italy*; orcid.org/0000-0001-5952-9927

Complete contact information is available at: https://pubs.acs.org/10.1021/acsomega.0c05168

Notes

The authors declare no competing financial interest.

ACKNOWLEDGMENTS

This work has been funded by a grant from the American University in Cairo to Prof. H.M.E.-S.A.

REFERENCES

(1) Galanski, M.; Jakupec, M.; Keppler, B. Update of the preclinical situation of anticancer platinum complexes: novel design strategies and innovative analytical approaches. *Curr. Med. Chem.* **2005**, *12*, 2075−2094.

(2) Harper, B. W.; Krause-Heuer, A. M.; Grant, M. P.; Manohar, M.; Garbutcheon-Singh, K. B.; Aldrich-Wright, J. R. Advances in platinum chemotherapeutics. *Chem. —Eur J.* **2010**, *16*, 7064−7077.

(3) Wong, E.; Giandomenico, C. M. Current Status of Platinum-Based Antitumor Drugs. *Chem. Rev.* **1999**, *99*, 2451−2466.

(4) Jakupec, M. A.; Galanski, M.; Keppler, B. K. Tumour-inhibiting platinum complexes-state of the art and future perspectives. *Rev. Physiol. Biochem. Pharmacol.* **2003**, *146*, 1−53.

(5) Wheate, N. J.; Walker, S.; Craig, G. E.; Oun, R. The status of platinum anticancer drugs in the clinic and in clinical trials. *Dalton Trans.* **2010**, *39*, 8113−8127.

(6) Arango, D.; Wilson, A. J.; Shi, Q.; Corner, G. A.; Arañes, M. J.; Nicholas, C.; Lesser, M.; Mariadason, J. M.; Augenlicht, L. H. Molecular mechanisms of action and prediction of response to oxaliplatin in colorectal cancer cells. *Br. J. Cancer* **2004**, *91*, 1931−1946.

(7) Kweekel, D.; Gelderblom, H.; Guchelaar, H. Pharmacology of oxaliplatin and the use of pharmacogenomics to individualize therapy. *Canc. Treat Rev.* **2005**, *31*, 90−105.

(8) Montagnani, F.; Turrisi, G.; Marinozzi, C.; Aliberti, C.; Fiorentini, G. Effectiveness and safety of oxaliplatin compared to cisplatin for advanced, unresectable gastric cancer: a systematic review and meta-analysis. *Gastric Cancer* **2011**, *14*, 50−55.

(9) Kawai, Y.; Taniuchi, S.; Okahara, S.; Nakamura, M.; Gemba, M. Relationship between Cisplatin or Nedaplatin-Induced Nephrotoxicity and Renal Accumulation. *Biol. Pharm. Bull.* **2005**, *28*, 1385−1388.

(10) El-Shafie, S.; Fahmy, S. A.; Ziko, L.; Elzahed, N.; Shoeib, T.; Kakarougkas, A. Encapsulation of Nedaplatin in Novel PEGylated Liposomes Increases Its Cytotoxicity and Genotoxicity against A549 and U2OS Human Cancer Cells. *Pharmaceutics* **2020**, *12*, 863.

(11) Fahmy, S. A.; Mamdouh, W. Garlic oil−loaded PLGA nanoparticles with controllable size and shape and enhanced antibacterial activities. *J. Appl. Polym. Sci.* **2018**, *135*, 46133.

(12) Dragovich, T.; Mendelson, D.; Kurtin, S.; Richardson, K.; Von Hoff, D.; Hoos, A. A Phase 2 trial of the liposomal DACH platinum L-NDDP in patients with therapy-refractory advanced colorectal cancer. *Canc. Chemother. Pharmacol.* **2006**, *58*, 759−764.

(13) Lu, C.; Perez-Soler, R.; Piperdi, B.; Walsh, G. L.; Swisher, S. G.; Smythe, W. R.; Shin, H. J.; Ro, J. Y.; Feng, L.; Truong, M.; Yalamanchili, A.; Lopez-Berestein, G.; Hong, W. K.; Khokhar, A. R.; Shin, D. M. Phase II study of a liposome-entrapped cisplatin analog (L-NDDP) administered intrapleurally and pathologic response rates in patients with malignant pleural mesothelioma. *J. Clin. Oncol.* **2005**, *23*, 3495−3501.

(14) Koshkaryev, A.; Sawant, R.; Deshpande, M.; Torchilin, V. Immunoconjugates and long circulating systems: origins, current state of the art and future directions. *Adv. Drug Deliv. Rev.* **2013**, *65*, 24−35.

(15) Boulikas, T.; Pantos, A.; Bellis, E.; Christofis, P. Designing platinum compounds in cancer: structures and mechanisms (review). *Cancer Ther.* **2007**, *5*, 537−583.

(16) Fahmy, SA.; Brüßler, J.; Alawak, M.; El-Sayed, M. M. H.; Bakowsky, U.; Shoeib, T. Chemotherapy Based on Supramolecular Chemistry:A Promising Strategy in Cancer Therapy. *Pharmaceutics* **2019**, *11*, 292.

(17) Cao, L.; Hettiarachchi, G.; Briken, V.; Isaacs, L. Cucurbit[7]uril containers for targeted delivery of oxaliplatin to cancer cells. *Angew. Chem.* **2013**, *52*, 12033−12037.

(18) Chen, Y.; Huang, Z.; Zhao, H.; Xu, J.-F.; Sun, Z.; Zhang, X. Supramolecular Chemotherapy: Cooperative Enhancement of Anti-tumor Activity by Combining Controlled Release of Oxaliplatin and Consuming of Spermine by Cucurbit[7]uril. *ACS Appl. Mater. Interfaces* **2017**, *9*, 8602−8608.

(19) Jeon, Y. J.; Kim, S. Y.; Ko, Y. H.; Sakamoto, S.; Yamaguchi, K.; Kim, K. Novel molecular drug carrier: encapsulation of oxaliplatin in cucurbit[7]uril and its effects on stability and reactivity of the drug. *Org. Biomol. Chem.* **2005**, *3*, 2122−2125.

(20) Plumb, J. A.; Venugopal, B.; Oun, R.; Gomez-Roman, N.; Kawazoe, Y.; Venkataramanan, N. S.; Wheate, N. J. Cucurbit[7]uril encapsulated cisplatin overcomes cisplatin resistance via a pharmaco-kinetic effect. *Metallomics* **2012**, *4*, 561−567.

(21) Guo, D.-S.; Liu, Y. Supramolecular Chemistry of p-Sulfonatocalix[n]arenes and Its Biological Applications. *Chem. Res.* **2014**, *47*, 1925−1934.

(22) Coleman, A. W.; Jebors, S.; Cecillon, S.; Perret, P.; Garin, D.; Marti-Battle, D.; Moulin, M. Toxicity and biodistribution of para-sulfonato-calix[4]arene in mice. *New J. Chem.* **2008**, *32*, 780−782.
(23) Fahmy, S. A.; Ponte, F.; El-Rahman, M. K. A.; Russo, N.; Sicilia, E.; Shoeib, T. Investigation of the host-guest complexation between 4-sulfocalix [4] arene and nedaplatin for potential use in drug delivery. *Spectrochim. Acta, Part A* **2018**, *193*, 528−536.
(24) Wheate, N. J. Improving platinum(II)-based anticancer drug delivery using cucurbit[n]urils. *J. Inorg. Biochem.* **2008**, *102*, 2060−2066.
(25) Wheate, N. J.; Abbott, G. M.; Tate, R. J.; Clements, C. J.; Edrada-Ebel, R.; Johnston, B. F. Side-on binding of p-sulphonatocalix[4]arene to the dinuclear platinum complex trans-$[\{PtCl(NH_3)_2\}_2$mu-dpzm$]^{2+}$ and its implications for anticancer drug delivery. *J. Inorg. Biochem.* **2009**, *103*, 448−454.
(26) Guo, D.-S.; Uzunova, V. D.; Su, X.; Liu, Y.; Nau, W. M. Operational calixarene-based fluorescent sensing systems for choline and acetylcholine and their application to enzymatic reactions. *Chem. Sci.* **2011**, *2*, 1722−1734.
(27) Shinkai, S.; Araki, K.; Matsuda, T.; Manabe, O. NMR Determination of Association Constants for Aqueous Calixarene Complexes and Guest Template Effects on the Conformational Freedom. *Bull. Chem. Soc. Jpn.* **1989**, *62*, 3856−3862.
(28) Nebsen, M.; Abd El-Rahman, M. K.; Salem, M. Y.; El-Kosasy, A. M.; El-Bardicy, M. G. Stability-indicating spectrophotometric and spectrodensitometric methods for the determination of diacerein in the presence of its degradation product. *Drug Test. Anal.* **2011**, *3*, 221.
(29) Bosque-Sendra, J. M.; Almansa-López, E.; García-campaña, M.; Cuadros-rodríguez, L. Data Analysis in the Determination of Stoichiometries and Stability Constants of Complexes. *Anal. Sci.* **2003**, *19*, 1431−1439.
(30) Carvalho, C. P.; Uzunova, V. D.; Da Silva, J. P.; Nau, W. M.; Pischel, U. A photoinduced pH jump applied to drug release from cucurbit[7]uril. *Chem. Commun.* **2011**, *47*, 8793−8795.
(31) Marquez, C.; Nau, W. M. Two Mechanisms of Slow Host-Guest Complexation between Cucurbit[6]uril and Cyclohexylmethylamine: pH-Responsive Supramolecular Kinetics. *Angew. Chem., Int. Ed.* **2001**, *40*, 3155−3160.
(32) Miskolczy, Z.; Biczók, L. Photochromism in Cucurbit[8]uril Cavity: Inhibition of Hydrolysis and Modification of the Rate of Merocyanine−Spiropyran Transformations. *J. Phys. Chem. B* **2011**, *115*, 12577−12583.
(33) Wu, J.; Isaacs, L. Cucurbit[7]uril Complexation Drives Thermal trans−cis-Azobenzene Isomerization and Enables Colorimetric Amine Detection. *Chem. —Eur J.* **2009**, *15*, 11675−11680.
(34) Pischel, U.; Uzunova, V. D.; Remón, P.; Nau, W. M. Supramolecular logic with macrocyclic input and competitive reset. *Chem. Commun.* **2010**, *46*, 2635−2637.
(35) Praetorius, A.; Bailey, D. M.; Schwarzlose, T.; Nau, W. M. Design of a Fluorescent Dye for Indicator Displacement from Cucurbiturils: A Macrocycle-Responsive Fluorescent Switch Operating through a pK_a Shift. *Org. Lett.* **2008**, *10*, 4089−4092.
(36) Koner, A. L.; Nau, W. M. Cucurbituril Encapsulation of Fluorescent Dyes. *Supramol. Chem.* **2007**, *19*, 55−66.
(37) Arantes, L. M.; Varejão, E. V. V.; Pelizzaro-Rocha, K. J.; Cereda, C. M. S.; de Paula, E.; Lourenço, M. P.; Duarte, H. A.; Fernandes, S. A. Benzocaine Complexation with p-Sulfonic Acid Calix[n]arene: Experimental (^{1}H-NMR) and Theoretical ApproachesChem. *Chem. Biol. Drug Des.* **2014**, *83*, 550−559.
(38) Wheate, N. J.; Abbott, G. M.; Tate, R. J.; Clements, C. J.; Edrada-Ebel, R.; Johnston, B. F. Side-on binding of p-sulphonatocalix[4]arene to the dinuclear platinum complex trans-$[\{PtCl(NH_3)_2\}_2\mu$-dpzm$]^{2+}$ and its implications for anticancer drug delivery. *J. Inorg. Biochem.* **2009**, *103*, 448−454.
(39) Bakirci, H.; Koner, A. L.; Schwarzlose, T.; Nau, W. M. Analysis of host-assisted guest protonation exemplified for p-sulfonatocalix[4]-arene–towards enzyme-mimetic pKa shifts. *Chem. —Eur J.* **2006**, *12*, 4799−4807.
(40) Wang, G.-S.; Zhang, H.-Y.; Ding, F.; Liu, Y. Preparation and characterization of inclusion complexes of topotecan with sulfonato-calixarene. *J. Inclusion Phenom. Macrocyclic Chem.* **2011**, *69*, 85−89.
(41) Yang, W.; De Villiers, M. Effect of 4-Sulphonato-Calix[n]Arenes and Cyclodextrins on the Solubilizationof Niclosamide, a Poorly Water Soluble Anthelmintic. *AAPS J.* **2005**, *7*, No. E241.
(42) Zhang, D.; Zhang, J.; Jiang, K.; Li, K.; Cong, Y.; Pu, S.; Jin, Y.; Lin, J. Preparation, characterisation and antitumour activity of β-, γ-and HP-β-cyclodextrin inclusion complexes of oxaliplatin. *Spectrochim. Acta, Part A* **2016**, *152*, 501−508.
(43) Fahmy, S. A.; Brüßler, J.; Ponte, F.; Abd El-Rahman, M. K.; Russo, N.; Sicilia, E.; Bakowsky, U.; Shoeib, T. A study on the physicochemical properties and cytotoxic activity of p-sulfocalix[4]-arene-nedaplatin complex. *J. Phys.: Conf. Ser.* **2019**, *1310*, 012011.
(44) Legault, C. Y. CYLview, 1.0b. Universite de Sherbrooke. 2009. http://www.cylview.org.web
(45) El-Rahman, M. K.; Mazzone, G.; Mahmoud, A. M.; Sicilia, E.; Shoeib, T. Spectrophotometric determination of choline in pharmaceutical formulations via host-guest complexation with a biomimetic calixarene receptor. *Microchem. J.* **2019**, *146*, 735−741.
(46) T. A., Keith *AIMAll*, version 17.11.14; TK Gristmill Software: Overland Park KS, USA, 2017. aim.tkgristmill.com.
(47) Bader, R. F. W.; Essén, H. The Characterization of Atomic Interactions. *Chem. Phys.* **1984**, *80*, 1943−1960.
(48) Shahi, A.; Arunan, E. Hydrogen bonding, halogen bonding and lithium bonding: an atoms in molecules and natural bond orbital perspective towards conservation of total bond order, inter- and intra-molecular bonding. *Phys. Chem. Chem. Phys.* **2014**, *16*, 22935−22952.
(49) Skehan, P.; Storeng, R.; Scudiero, D.; Monks, A.; McMahon, J.; Vistica, D.; Warren, J. T.; Bokesch, H.; Kenney, S.; Boyd, M. R. New Colorimetric Cytotoxicity Assay for Anticancer-Drug Screening. *J. Natl. Cancer Inst.* **1990**, *82*, 1107−1112.
(50) Allam, R. M.; Al-Abd, A. M.; Khedr, A.; Sharaf, O. A.; Nofal, S. M.; Khalifa, A. E.; Mosli, H. A.; Abdel-Naim, A. B. Fingolimod interrupts the cross talk between estrogen metabolism and sphingolipid metabolism within prostate cancer cells. *Toxicol. Lett.* **2018**, *291*, 77−85.
(51) Vichai, V.; Kirtikara, K. Sulforhodamine B colorimetric assay for cytotoxicity screening. *Nat. Protoc.* **2006**, *1*, 1112−1116.
(52) Frisch, M. J.; Trucks, G. W.; Schlegel, H. B.; Scuseria, G. E.; Robb, M. A.; Cheseman, J. R.; Scalmani, G.; Barone, V.; Mennucci, B.; Petersson, G. A.; Nakatsuji, H.; Caricato, H.; Li, X.; Hratchian, H. P.; Izmaylov, A. F.; Bloino, J.; Zheng, G.; Sonnerberg, J. L.; Hada, M.; Ehara, M.; Toyota, K.; Fukuda, R.; Hasegawa, J.; Ishida, M.; Nakajima, T.; Honda, Y.; Kitao, O.; Nakai, H.; Vreven, T.; Montgomery, J. A.; Peralta, J. E.; Ogliaro, F.; Bearpark, M.; Heyd, J. J.; Brothers, E.; Kudin, K. N.; Staroverov, V. N.; Kobayashi, R.; Normand, J.; Raghavachari, K.; Rendell, A.; Burant, J. C.; Iyengar, S. S.; Tomasi, J.; Cossi, M.; Nega, R.; Millam, J. M.; Klene, M.; Knox, J. E.; Cross, J. B.; Bakken, V.; Adamo, C.; Jaramillo, J.; Gomperts, R.; Stratmann, R. E.; Yazyev, O.; Austin, A. J.; Cammi, R.; Pomelli, C.; Ochterski, J. W.; Martin, R. L.; Morokuma, K.; Zakrzewski, V. G.; Voth, G. A.; Salvador, P.; Dannenberg, J. J.; Daprich, S.; Daniels, A. D.; Farkas, A.; Foreaman, J. B.; Ortiz, J. V.; Cioslowski, J.; Fox, D. J. *Gaussian 09*, Revision A.02, Revision D.01; Gaussian; Inc.; Wallingford, CT, 2009.
(53) Grimme, S. Semiempirical GGA-type density functional constructed with a long-range dispersion correction. *J. Comput. Chem.* **2006**, *27*, 1787−1799.
(54) Andrae, D.; Häusermann, U.; Dolg, M.; Stoll, H.; Preuss, H. Energy-adjustedab initio pseudopotentials for the second and third row transition elements. *Theor. Chim. Acta* **1990**, *77*, 123.
(55) Cossi, M.; Barone, V. Solvent effect on vertical electronic transitions by the polarizable continuum model. *J. Chem. Phys.* **2000**, *112*, 2427−2435.
(56) Boys, S. F.; Bernardi, F. The calculation of small molecular interactions by the differences of separate total energies. Some procedures with reduced errors. *Mol. Phys.* **1970**, *19*, 553.

https://dx.doi.org/10.1021/acsomega.0c05168
ACS Omega 2020, 5, 31456−31466

(57) Guex, N.; Peitsch, M. C. SWISS-MODEL and the Swiss-PdbViewer: An environment for comparative protein modeling. *Electrophoresis* **1997**, *18*, 2714−2723.
(58) Bader, R. F. W. A quantum theory of molecular structure and its applications. *Chem. Rev.* **1991**, *91*, 893−928.

https://dx.doi.org/10.1021/acsomega.0c05168
ACS Omega 2020, 5, 31456−31466